

## ROLE OF ROTATIONAL TRANSFORM AND ENHANCED HALL EFFECT IN ALFVÉN WAVE ANTENNA OPTIMIZATION

Satish Puri

MPI für Plasmaphysik, EURATOM Association, Garching bei München, FRG

Modifications in the Alfvén wave heating contributed by the plasma equilibrium current through the rotational transform and the enhanced Hall effect are studied in a model that includes electron Landau damping. Optimum coupling with  $R \approx 0.7\Omega$  occurs for  $n = 8$  and is not significantly affected by the equilibrium current. The antenna  $Q \approx 17$  is comparable to the ICRF antennas, while the surface heating is negligibly small. For the large  $n \sim 8$  values, mode splitting due to the removal of the poloidal degeneracy combined with the finite electron temperature effects leads to significant broadening of the energy absorption profile. No evidence of discrete Alfvén wave (DAW) excitation is observed. An approximate analysis is presented to highlight the dominant role played by the density gradient term *vis a vis* the enhanced Hall term in the determination of the plasma surface impedance, and consequently the antenna loading.

### 1. INTRODUCTION

Efficient coupling to the Alfvén waves requires (i) conditions conducive to high conversion efficiency, and (ii) minimization of the evanescence between the plasma edge and the singular surface,  $\gamma_1 = \epsilon_x - n_z^2 = 0$ . The first of these conditions demands the choice of a large  $\omega/\omega_{ci}$  ratio requiring a high toroidal number  $n$ , whereas the second condition is best satisfied at low frequencies and therefore for low values of  $n$ . Although this predicament has been recognized previously, the precise quantitative implications were brought to a focus in our recent antenna optimization study<sup>1</sup>. It was shown that optimal coupling, possessing high efficiency and low  $Q$  necessary for thermonuclear applications, would not be feasible with the low antenna toroidal wave number,  $N \sim 2$  employed in the current experimental practice; acceptable coupling may require using  $N \sim 8$ , where  $N = N_A/2$ ,  $N_A$  being the number of alternately phased antenna sections along the torus circumference. The role of the equilibrium current (introduced through the safety factor  $q$ ) in the antenna optimization is addressed in this paper.

The Alfvén resonance relation in the local coordinates<sup>2</sup>

$$\epsilon_\xi = n_\xi^2 = \cos^2 \chi n_z^2 \left( 1 + \frac{m}{nq} \right)^2, \quad (1)$$

where  $\chi$  is the angle between the magnetic field and the cylindrical axis, involves both the poloidal ( $m$ ) and the toroidal ( $n$ ) wave numbers, causing a multiplicity of radially distributed resonances for a given  $n$ . In cylindrical geometry, the Doppler shifted frequency seen by the electrons causes an enhancement of the Hall term by the factor

$$\left| \frac{\tilde{\epsilon}_y}{\epsilon_y} \right| \approx \frac{2}{qk_0 r_T} \frac{\omega_{ci}^2}{\omega \omega_{pi}} \gg 1. \quad (2)$$

In addition, the rf current accompanying the enhanced Hall effect gives rise to MHD kink modes, also known as the discrete Alfvén waves<sup>2</sup>.

## 2. THE COMPUTATIONAL RESULTS

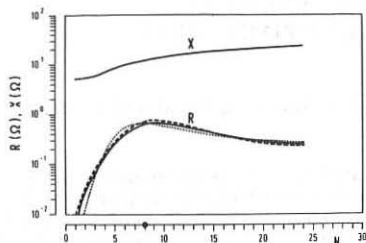


Fig.1

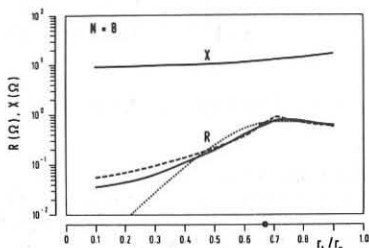


Fig.2

Figure 1 shows the antenna loading in the absence of the plasma current (dotted curve), with rotational transform alone (dashed curve) and with the addition of the enhanced Hall effect (solid curve), using the ASDEX UPGRADE parameters<sup>3</sup> with  $q = 1$  at the axis and  $q = 3$  at the surface. The equilibrium current produces insignificant changes in the Alfvén wave antenna loading provided a fixed position is maintained for the principal resonance corresponding to  $m = \mp 1$ ,  $n/|n| = \pm 1$ . The rotational transform does, however, contribute (Fig. 2) to an increased antenna loading for lower values of  $r_A/r_p$ , owing to the presence of parasitic resonances occurring closer to the plasma boundary. This effect is further magnified<sup>2</sup> if the position of the secondary resonance corresponding to  $m = \pm 1$ ,  $n/|n| = \pm 1$  were to be held fixed, so that the principal resonance with  $m = \mp 1$  itself assumes the role of a parasitic mode.

## 3. PLASMA SURFACE IMPEDANCE

The approximate differential equation for the fast wave propagation in the slab plasma model (including the enhanced Hall effect) may be written as<sup>4</sup>

$$\mathcal{E}_y'' + k_x^2(x)\mathcal{E}_y = 0, \quad (3)$$

where  $E_y = (\gamma_2/\gamma_1)^{1/2}\mathcal{E}_y$ ,  $\gamma_2 = \gamma_1 - n_y^2$ ,

$$k_x^2(x) = \frac{\gamma_1^2 - \tilde{\epsilon}_y^2}{\gamma_1} k_0^2 - k_y^2 + k_g^2, \quad (4)$$

$$\begin{aligned} k_x^2(x) &= \frac{n_y^2}{\gamma_1 \gamma_2} \left[ .5\epsilon_x'' - \frac{\gamma_1 - .25n_y^2}{\gamma_1 \gamma_2} \epsilon_x'^2 - \frac{\tilde{\epsilon}_y}{n_y} k_0 \epsilon_x' + \frac{\gamma_2}{n_y} k_0 \tilde{\epsilon}_y' \right] \\ &\approx -\frac{n_y^2}{(\gamma_1 \gamma_2)^2} (\gamma_1 - .25n_y^2) \epsilon_x'^2. \end{aligned} \quad (5)$$

The three terms in (4) are the contributions from the uniform plasma, the finite  $k_y$ , and the gradient effects, respectively. The cutoffs occurring at the zeros of  $k_x$  are profoundly

affected by the finite  $k_y$  and the gradient terms. The presence of the  $k_y^2$  term has the effect of moving the right cutoff away from the resonance region thereby diminishing the coupling to the propagating branch of the compressional mode. Both  $k_y$  and  $k_g$  cause a shift in the left cutoff, significantly shrinking the evanescent region and thus improving the antenna loading. An exception occurs for the  $m = 0$  case when the cutoff positions are dictated by the Hall term  $\tilde{\epsilon}_y$  alone. The zeros of  $k_x$  are approximately given by

$$(\gamma_1^2 - \tilde{\epsilon}_y^2) - \gamma_1 n_y^2 - \frac{n_y^2}{\gamma_1 \gamma_2^2} (\gamma_1 - .25 n_y^2) \left( \frac{\epsilon'_x}{k_0} \right)^2 = 0. \quad (6)$$

Assuming that  $n_y^2 \gg \gamma_1$  in the critical region surrounding the resonance, reduces (6) to

$$\gamma_1^2 + \left( \frac{\tilde{\epsilon}_y}{n_y} \right)^2 \gamma_1 - \frac{1}{4} \left( \frac{\epsilon'_x}{k_0 n_y} \right)^2 = 0. \quad (7)$$

The cutoffs correspond to

$$\gamma_1 \approx \pm \frac{1}{2} \frac{\epsilon'_x}{k_0 n_y} - \frac{1}{2} \left( \frac{\tilde{\epsilon}_y}{n_y} \right)^2. \quad (8)$$

The two terms on the right hand side of (8) originate from the gradient and the enhanced Hall effect, respectively. Their ratio

$$\mathcal{R} = \frac{n_y \epsilon'_x}{k_0 \tilde{\epsilon}_y^2} \approx \left( \frac{qr_T}{2r_p} \right)^2 = \left( \frac{qA}{2} \right)^2 \gg 1, \quad (9)$$

( $A$  is the aspect ratio) shows the dominant role played by the gradient effects *vis a vis* the enhanced Hall effect in the location of the cutoffs and hence on the coupling itself.

We may now approximately refactor (4) into the form

$$k_x^2(x) = k_0^2 (n_z^2 - 1) \frac{x_0 (x - x_{c1})(x - x_{c2})}{x_{c1} x_{c2} (x - x_0)}. \quad (10)$$

For the large  $k_y^2 \sim r_p^{-2}$  encountered in the  $m \neq 0$  case, the cutoff at  $x_{c2}$  is well removed from the resonance region so that

$$k_x^2(x) \approx -\alpha k_0^2 \frac{x - x_{c1}}{x - x_0}, \quad (11)$$

where  $\alpha = (n_z^2 - 1)x_0/x_{c1}$ . Using (11) reduces (3) to the Whittaker equation

$$\frac{\partial^2 \mathcal{E}}{\partial \gamma^2} + k_0^2 \left( -\frac{1}{4} - \frac{1}{2} \frac{\beta}{\gamma} \right) \mathcal{E} = 0, \quad (12)$$

where  $\beta = \alpha^{1/2} k_0 (x_0 - x_{c1})$  and  $\gamma = 2\alpha^{1/2} k_0 (x - x_0)$ . Discarding growing solutions, one obtains from (12)

$$E_y = \left( \frac{\gamma_2}{\gamma_1} \right)^{1/2} W_{\kappa, \mu}(\gamma), \quad (13)$$

where  $W_{\kappa, \mu}(\gamma)$  is the Whittaker function<sup>5</sup>,  $\mu = 1/2$  and  $\kappa = -\beta/2$ . Using the relations  $H_z = -i(\gamma_1/\gamma_2)(\partial E_y/\partial x)$ ,  $\zeta_f = E_y(0)/H_z(0)$  and  $n_{yz}^2 = n_y^2 + n_z^2$  yields

$$\zeta_f = ik_0 x_0 \frac{n_{yz}^2 - 1}{n_z^2 - 1} \left[ \frac{.5n_y^2}{n_{yz}^2 - 1} + .5\alpha^{1/2} k_0(x_0 + x_{c1}) + \frac{U(.5\beta, 2, \gamma)}{U(1 + .5\beta, 2, \gamma)} \right]^{-1}, \quad (14)$$

where  $U(a, n + 1, \gamma)$  is the logarithmic solution of the Kummer equation given by<sup>5</sup>

$$U(a, n + 1, \gamma) = \frac{(-1)^{n+1}}{n! \Gamma(a - n)} \left[ \Phi(a, n + 1, \gamma) \ln \gamma + \sum_{r=0}^{\infty} \frac{(a)_r \gamma^r}{(n + 1)_r r!} \times \right. \\ \left. \{ \psi(a + r) - \psi(1 + r) - \psi(1 + n + r) \} \right] + \sum_1^n \frac{(n - 1)!}{\Gamma(a)} \gamma^{-n} \Phi(a - n, 1 - n, \gamma), \quad (15)$$

where,  $\Phi(a, n + 1, \gamma)$  is the Kummer function of the first kind,  $\Gamma(a)$  is the gamma function,  $\psi(a) = \Gamma'(a)/\Gamma(a)$  and  $(a)_n = a(a + 1)(a + 2) \dots (a + n - 1)$ ,  $(a)_0 = 1$ .

Since for  $x = 0$ ,  $\gamma = -2\alpha^{1/2} k_0 x_0$  is a negative quantity,  $\ln \gamma$  in (15) contributes an imaginary part which gives rise to the resistive component of  $\zeta_f$  in (14). For  $\omega/\omega_{ci} \rightarrow 0$ ,  $\beta \rightarrow 0$  so that  $[\Gamma(a - n)]^{-1} \rightarrow 0$  and the resistive loading disappears. For a fixed value of  $\alpha$ , increasing  $\omega/\omega_{ci}$  causes a rapid increase in  $\beta$  due to the increasing  $k_0$  and  $(x_0 - x_{c1})$ . This, in turn, causes a steep rise in the loading resistance as  $[\Gamma(a - n)]^{-1}$  as well as  $\Phi(a, n + 1, \gamma)$  increase. The net result is a marked improvement in the conversion efficiency leading to the superior coupling properties at larger values of  $\omega/\omega_{ci}$  and hence at higher toroidal wave numbers.

The analysis presented here is approximate without pretense to quantitative accuracy, while the term *cutoff* is employed figuratively. Nevertheless, a credible picture of the physical processes involved emerges and the salient features of Alfvén wave coupling are in qualitative agreement with the computed results of Figs. 1 and 2.

#### 4. DISCUSSION AND CONCLUSIONS

No deliberate attempt either to include or to exclude the DAW resonances was made during the course of these computations. However, over the broad range of parameters studied, no evidence of pronounced irregularities in the antenna loading characteristics are observed. These results indicate that an inadvertent excitation of DAW, attended by uncertain consequences, constitutes no particular cause for concern. One may conclude that the presence of plasma equilibrium current leaves the Alfvén wave antenna coupling substantially unaffected. The existence of moderate  $Q$ , and the freedom from serious surface heating effects<sup>3</sup> present a strong case for Alfvén wave heating.

#### REFERENCES

- 1 S. Puri, Nucl. Fusion **27**, 229 (1987).
- 2 K. Appert, B. Balet and J. Vaclavik, Phys. Lett. **87A**, 233 (1982).
- 3 S. Puri in the Proceedings of the 7th APS Topical Meeting on the Application of radio frequency Power to Plasmas, Kissimmee, Florida (1987).
- 4 S. Puri, Phys. Fluids **27**, 2156 (1984).
- 5 L. J. Slater in Handbook of Mathematical Functions, (M. Abramowitz and I. A. Stegun, Eds), National Bureau of Standards, U. S. Dept. of Commerce, Washington, D. C., 1964.